

Genome-wide DNA methylation analysis in hepatocellular carcinoma

NOBUHISA YAMADA¹, KOHICHIROH YASUI¹, OSAMU DOHI¹, YASUYUKI GEN¹, AKIRA TOMIE¹,
TOMOKO KITAICHI¹, NAOTO IWAI¹, HIRONORI MITSUYOSHI¹, YOSHIO SUMIDA¹, MICHIHISA MORIGUCHI¹,
KANJI YAMAGUCHI¹, TAICHIRO NISHIKAWA¹, ATSUSHI UMEMURA¹, YUJI NAITO¹,
SHINJI TANAKA^{2,3}, SHIGEKI ARII^{2,4} and YOSHITO ITOH¹

¹Department of Molecular Gastroenterology and Hepatology, Graduate School of Medical Science, Kyoto Prefectural University of Medicine, Kyoto 602-8566; Departments of ²Hepato-Biliary-Pancreatic Surgery and ³Molecular Oncology, Tokyo Medical and Dental University, Tokyo 113-8510; ⁴Hamamatsu Rosai Hospital, Japan Labour Health and Welfare Organization, Hamamatsu 430-8525, Japan

Received June 11, 2015; Accepted November 3, 2015

DOI: 10.3892/or.2016.4619

Abstract. Epigenetic changes as well as genetic changes are mechanisms of tumorigenesis. We aimed to identify novel genes that are silenced by DNA hypermethylation in hepatocellular carcinoma (HCC). We screened for genes with promoter DNA hypermethylation using a genome-wide methylation microarray analysis in primary HCC (the discovery set). The microarray analysis revealed that there were 2,670 CpG sites that significantly differed in regards to the methylation level between the tumor and non-tumor liver tissues; 875 were significantly hypermethylated and 1,795 were significantly hypomethylated in the HCC tumors compared to the non-tumor tissues. Further analyses using methylation-specific PCR, combined with expression analysis, in the validation set of primary HCC showed that, in addition to three known tumor-suppressor genes (*APC*, *CDKN2A*, and *GSTPI*), eight genes (*AKR1B1*, *GRASP*, *MAP9*, *NXPE3*, *RSPH9*, *SPINT2*, *STEAP4*, and *ZNF154*) were significantly hypermethylated and down-regulated in the HCC tumors compared to the non-tumor liver tissues. Our results suggest that epigenetic silencing of these genes may be associated with HCC.

Introduction

Hepatocellular carcinoma (HCC) is the third leading cause of cancer-related death worldwide (1). It is estimated to cause approximately half a million deaths annually. Several risk

factors for HCC have been reported, including infection with hepatitis B and hepatitis C viruses, dietary intake of aflatoxin, and alcohol consumption. However, the molecular pathogenesis of HCC is not fully understood.

Epigenetic changes are the mechanisms of tumorigenesis as well as genetic changes such as chromosomal alterations, gene amplifications, deletions, and mutations. DNA methylation of CpG islands within the promoter regions of tumor-suppressor genes is known to inhibit transcriptional initiation, and thereby silence these genes. Tumor-suppressor genes that are frequently methylated in HCC include *APC* (2), *CDKN2A* (3), *RASSF1A* (4), and *GSTPI* (5). Aberrant DNA methylation of various tumor-suppressor genes is suggested to be correlates with biological features and clinical outcome of HCC (6,7).

In the present study, we aimed to identify novel genes that are silenced by DNA hypermethylation in HCC. We screened for genes with promoter DNA hypermethylation using a genome-wide methylation microarray analysis in primary HCC tumors by comparison with their non-tumor tissue counterparts. Further methylation analyses, combined with expression analyses, revealed novel genes that were down-regulated by aberrant promoter hypermethylation in HCC.

Materials and methods

Primary tumors and cell lines. Paired tumor and non-tumor tissues were obtained from HCC patients who underwent surgery at the Hospital of Tokyo Medical and Dental University. All specimens were immediately frozen in liquid nitrogen and were stored at -80°C until required. Table I summarizes the clinical characteristics of a total of 47 patients (20 in the discovery set and 27 in the validation set) in the present study. The protocol of this study was approved by the ethics committees and conducted in accordance with the Declaration of Helsinki. Informed consent was obtained from each patient.

Three HCC cell lines, SNU449, Li7 and HLF, were examined. All cell lines were maintained in Dulbecco's modified

Correspondence to: Dr Kohichiroh Yasui, Department of Molecular Gastroenterology and Hepatology, Graduate School of Medical Science, Kyoto Prefectural University of Medicine, 465 Kajii-cho, Kamigyo-ku, Kyoto 602-8566, Japan
E-mail: yasui@koto.kpu-m.ac.jp

Key words: epigenetics, DNA methylation, hepatocellular carcinoma

Eagle's medium (DMEM) supplemented with 10% fetal calf serum.

DNA extraction and bisulfite modification. Genomic DNA was isolated using the Puregene DNA isolation kit (Gentra, Minneapolis, MN, USA). Bisulfite modification of DNA was performed using an EZ DNA Methylation kit (Zymo Research, Irvine, CA, USA).

Illumina HumanMethylation27 BeadChip. Genome-wide DNA methylation was analyzed by the HumanMethylation27 BeadChip (Illumina, San Diego, CA, USA), according to the instructions from the manufacturer. This Illumina BeadChip interrogates 27,578 CpG sites, which were selected predominantly from the promoter regions of an annotated 14,475 genes. Data were analyzed using Illumina GenomeStudio software. Methylation values are expressed as a β -value (between 0 and 1) for each CpG site, representing a continuous measurement from 0 (completely unmethylated) to 1 (completely methylated).

Differential methylation was assessed by comparing the mean methylation level (β -value) of HCC tumor tissues with the mean β -value of non-tumor liver tissues. Selection of significantly differentially methylated loci was based on i) a β -value difference [Δ β] of at least 0.15 between HCC tumor and non-tumor samples and ii) a p-value of <0.01 as determined by paired t-test with false-discovery rate (FDR) correction for multiple comparisons, based on the Benjamini and Hochberg procedure (8).

Quantitative reverse transcription-polymerase chain reaction (qRT-PCR). Total RNA was obtained using TRIzol reagent (Invitrogen, Carlsbad, CA, USA). qRT-PCR experiments were performed with the LightCycler system using FastStart DNA Master Plus SYBR Green I (Roche Diagnostics, Penzberg, Germany), as previously described (9). The primers used are listed in Table II. The endogenous control for mRNA was *ACTB*.

Methylation-specific PCR (MSP). MSP was performed, as previously described (10). Briefly, genomic DNA was treated with sodium bisulfite and subjected to PCR using specific primer sets (Table II).

Combined bisulfite and restriction analysis (COBRA). COBRA was performed, as previously described (10). Briefly, genomic DNA was treated with sodium bisulfite and subjected to PCR using primers (Table II) designed to amplify a region from -97 to +239 bp relative to the transcription start site of *STEAP4*. The PCR products were digested with HpyCH4IV, which recognizes sequences unique to the methylated alleles, but cannot recognize unmethylated alleles, and the digested products were electrophoresed on 3% agarose gels and stained with ethidium bromide. Methylation levels were calculated as the ratio of the gray scale value of the methylated band to that of the combined methylated and unmethylated bands. The gray scale value was obtained by scanning the gel with Adobe Photoshop CS3 Extended software (Adobe Systems Incorporated, San Jose, CA, USA). Methylated and unmethylated bisulfite-converted control DNA (EpiTect control DNA

Table I. Patient characteristics.

Characteristics	Discovery set (n=20)	Validation set (n=27)
Age (years)	65.4±7.6	64.0±9.3
Gender		
Male	15	22
Female	5	5
Etiology		
Hepatitis B	3	5
Hepatitis C	11	14
Other	6	8
No. of HCC tumors		
Single	10	15
Multiple	10	12
Maximum tumor size (cm)	5.9±3.0	7.0±4.8
Child-Pugh class (A/B/C)	20/0/0	27/0/0
Clinical stage (I/II/III/IVa/IVb) ^a	0/7/8/5/0	0/8/10/8/1
Background of the liver tissue		
Normal liver	2	2
Chronic hepatitis	6	11
Liver cirrhosis	12	14

Values are number or mean ± SD. Where no other unit is specified, values refer to the number of patients. ^aAccording to the staging system of the Liver Cancer Study Group of Japan.

set; Qiagen, Tokyo, Japan) served as controls for methylated and unmethylated DNA, respectively, in MSP and COBRA.

Drug treatment. Cells were treated with 1 or 5 μ M of 5-aza-2'-deoxycytidine (5-aza-dC; Sigma-Aldrich, St. Louis, MO, USA) for 4 days or 50 ng/ml of trichostatin A (TSA; Wako, Osaka, Japan) for 1 day. In assessing drug synergy, cells were cultured in the presence of 1 or 5 μ M of 5-aza-dC for 4 days, and were then treated for an additional 24 h with 50 ng/ml of TSA.

Immunohistochemistry. The HCC tissue microarray (US Biomax, Rockville, MD, USA) was analyzed for STEAP4 protein expression. Anti-STEAP4 polyclonal antibody (Proteintech, Chicago, IL, USA) was used at a dilution of 1:50. Immunostaining of STEAP4 was carried out with the EnVision+ system (Dako, Tokyo, Japan).

Statistical analyses. Fisher's exact probability test, paired t-test, and Wilcoxon signed-rank test were performed using SPSS 15.0 software (SPSS, Inc., Chicago, IL, USA). P-values of <0.05 were considered significant.

KEGG pathway analysis (11) was performed to identify biological pathways significantly enriched for differentially methylated genes using the functional annotation tool of the Database for Annotation Visualization and Integrated

Table II. Sequences of the PCR primers used in the study.

Purpose	Gene	Forward primer	Reverse primer
Quantitative RT-PCR	<i>ZNF154</i>	5'-GCCTGTACCGTGATGTGATG-3'	5'-TTTTTCTCCAAGGTGCTGCT-3'
	<i>MAP9</i>	5'-GGTAGGTGTTACCGGCTTCA-3'	5'-CTCAACTCAGGCACACTCCA-3'
	<i>SPINT2</i>	5'-GGAAGGGAGGGGAGACTATG-3'	5'-AGAAATCGATCAGCGAGGAA-3'
	<i>AKR1B1</i>	5'-ACCTCCCACAAGGATTACCC-3'	5'-GGCAAAGCAAAGTGAAGAG-3'
	<i>RSPH9</i>	5'-TTAAGCGCGACTACCGCTAT-3'	5'-TCCACTCTGTGCAGTTCAGG-3'
	<i>GRASP</i>	5'-TCGGCTTTGAGATCCAGACT-3'	5'-TCTGAGAACATTGCCTGACG-3'
	<i>STEAP4</i>	5'-CAGAACACACGCTCCTTCAA-3'	5'-CCAGCCTGGATGGTACCTAA-3'
	<i>NXPE3</i>	5'-TCTGCAGCTCAGAAAAGCAA-3'	5'-CTGTGCGATGAAAGTGGCTGA-3'
	<i>ACTB</i>	5'-GTCCACCTTCCAGCAGATGT-3'	5'-TGTTTTCTGCGCAAGTTAGG-3'
Methylation-specific PCR	<i>ZNF154</i> M	5'-ATGTTTTGCGTTGAACGTTAC-3'	5'-CTAAAATAACCGCCACGAAA-3'
	<i>ZNF154</i> U	5'-AGAATGTTTTGTGTTGAATGTTAT-3'	5'-AAACTAAAATAACCACCACAAAA-3'
	<i>MAP9</i> M	5'-GGTGGTTGTTTTAGCGATAC-3'	5'-TCCTAAACCGAACGAAAA-3'
	<i>MAP9</i> U	5'-TTGGGTGGTTGTTTTAGTGATAT-3'	5'-CAATCCTAAACCAACAAAAA-3'
	<i>SPINT2</i> M	5'-TTTAGGTGCGTTTAGGGTC-3'	5'-ACCAATAACGAACGCCTATT-3'
	<i>SPINT2</i> U	5'-GGGTTTAGGTGTGTTTAGGGTT-3'	5'-ACCAATAACAAACACCTATTAAA-3'
	<i>AKR1B1</i> M	5'-GGGTCGGTTTTGTAGAGATC-3'	5'-CGCTAAAACCCAAAATACG-3'
	<i>AKR1B1</i> U	5'-TGGGGTTGGTTTTGTAGAGATT-3'	5'-CACTAAAACCCAAAATACAAA-3'
	<i>RSPH9</i> M	5'-GGGTTTTAGTTTCGGATCGTC-3'	5'-ATAATCGACGACGAAACCAA-3'
	<i>RSPH9</i> U	5'-GTAGGGTTTTAGTTTGGAATTGT-3'	5'-ATAATCAACAACAAACCAAAAA-3'
	<i>GRASP</i> M	5'-TTATAAAGGGAGGCGATTTC-3'	5'-CGACGAAAAATCATAACTCC-3'
	<i>GRASP</i> U	5'-AGTTTATAAAGGGAGGTGATT-3'	5'-CAACAAAAATCATAACTCCAAC-3'
	<i>STEAP4</i> M	5'-GTATCGTTGGCGTTGGAC-3'	5'-GCGACGAAAAATTTACAAACA-3'
	<i>STEAP4</i> U	5'-GTATTGTTGGTGTGGAT-3'	5'-ACAACAAAAATTTACAAACA-3'
	<i>NXPE3</i> M	5'-GCGATAGTTGTAGTGTCGC-3'	5'-ACCCCCGACTACGATTAATA-3'
	<i>NXPE3</i> U	5'-GGGGTGATAGTTGTAGTGTGT-3'	5'-CAACCCCCAATACTACAATTAATA-3'
COBRA	<i>STEAP4</i>	5'-GGGATTTTTAGTTTGAATTTT-3'	5'-ATTTACAAACACCTATTCTTCAAT-3'

COBRA, combined bisulfite and restriction analysis; M, methylation-specific primer; U, unmethylation-specific primer.

Discovery (DAVID) version 6.7 (12,13). P-values were calculated using a modified Fisher's exact test (EASE score).

Results

Genome-wide DNA methylation profiling of primary HCC. To identify genes that are silenced by DNA hypermethylation in HCC, we compared DNA methylation profiles between paired tumor and non-tumor tissues from 20 patients with primary HCC (the discovery set) using Illumina HumanMethylation27 BeadChip. The array data have been submitted to NCBI GEO under accession number (GSE73003). The strategy of the present study is shown as a flowchart in Fig. 1.

Overall, the average methylation level was slightly but significantly higher in the HCC tumors than the matched non-tumor liver tissues (median β -value of 0.093 and 0.091 in HCC tumors and non-tumor liver tissues, respectively) (Fig. 2A). There were 2,670 CpG sites that significantly differed in regards to the methylation level between the tumor and non-tumor tissues ($\Delta\beta > 0.15$ and $P < 0.01$, see Materials and methods). Of these 2,670 CpG sites, 875 were significantly hypermethylated and 1,795 were

significantly hypomethylated in the HCC tumors compared to the non-tumor liver tissues.

Fig. 2B shows a heatmap of 2,670 significantly differentially methylated CpG sites between the HCC tumors and non-tumor liver tissues. Good separation of HCC tumors and non-tumor liver tissues was observed. While the HCC tumors showed a variation in methylation profiles, the non-tumor liver tissues did not.

KEGG pathway analysis was performed to identify biological pathways significantly enriched for the 695 hypermethylated genes corresponding to 875 CpG sites that were hypermethylated in the HCC tumors. Four KEGG pathways, including neuroactive ligand-receptor interaction, focal adhesion, vascular smooth muscle contraction, and systemic lupus erythematosus, were significantly enriched for hypermethylated genes (Table III).

Selection and validation of candidate methylated genes. We focused on further examination for the top 30 most hypermethylated genes in the HCC tumors compared to the non-tumor liver tissues (Table IV). The list of 30 genes included three known tumor-suppressor genes, *APC* (adenomatous polyposis

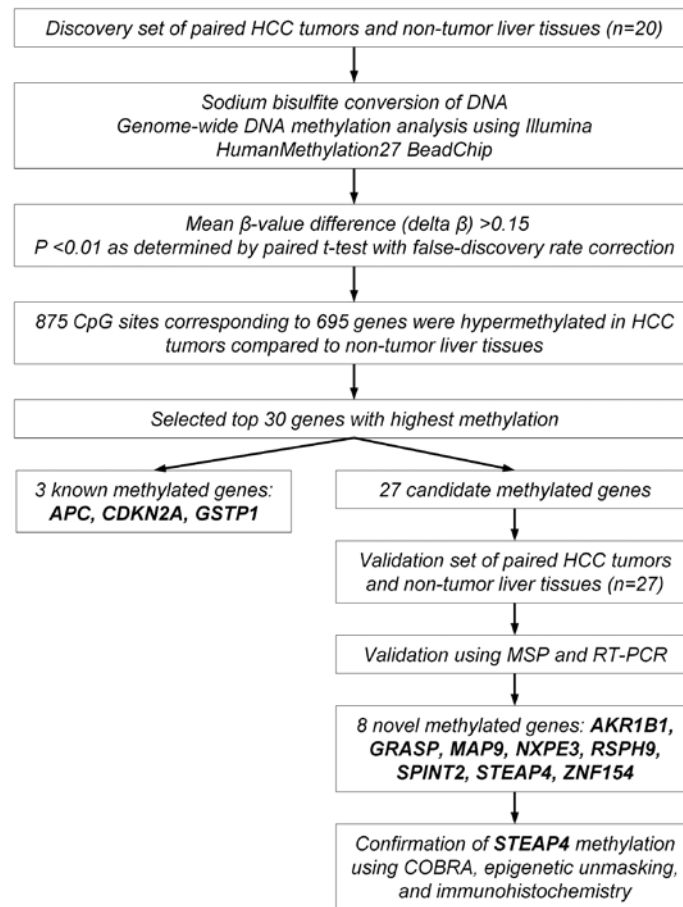


Figure 1. Schematic strategy for the identification of methylated genes in primary HCC. HCC, hepatocellular carcinoma; RT-PCR, real-time quantitative reverse transcription-polymerase chain reaction; MSP, methylation-specific PCR; COBRA, combined bisulfite and restriction analysis.

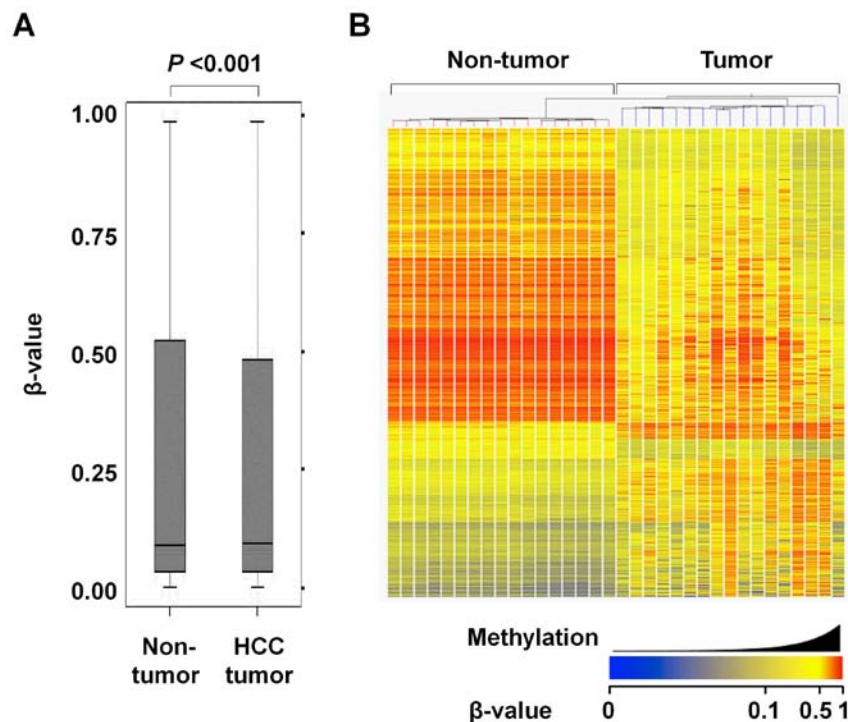


Figure 2. (A) Methylation levels as determined by Illumina HumanMethylation27 BeadChip in HCC tumors and non-tumor liver tissues. Methylation levels are expressed as a β -value, representing a continuous measurement from 0 (completely unmethylated) to 1 (completely methylated). The horizontal line is the mean; the box contains the values between the 25 and 75th percentiles; the error bars represent the range of data. (B) Hierarchical cluster analysis of 2,670 significantly differentially methylated CpG sites between the HCC tumors and non-tumor liver tissues. Hypermethylated and hypomethylated CpG sites are indicated by red and yellow, respectively.

Table III. KEGG pathways enriched for hypermethylated genes.

Pathway	Description	Count ^a	% ^b	P-value ^c	Fold enrichment
hsa04080	Neuroactive ligand-receptor interaction	22	3.19	0.001	2.08
hsa04510	Focal adhesion	17	2.46	0.008	2.05
hsa04270	Vascular smooth muscle contraction	11	1.59	0.016	2.38
hsa05322	Systemic lupus erythematosus	9	1.30	0.049	2.20

^aNumber of genes involved in the pathway; ^bpercentage of genes involved in the pathway; ^cEASE score, a modified Fisher's exact p-value, for gene-enrichment analysis.

Table IV. Top 30 hypermethylated genes in the HCC tumors^a.

Gene	Target ID	Mean β -value in non-tumors	Mean β -value in tumors	Mean β -value difference ($\Delta \beta$)	Corrected p-value ^b
<i>DNM3</i>	cg23391785	0.16	0.70	0.54	1.93E-06
<i>ZNF154</i>	cg21790626	0.08	0.62	0.54	1.67E-09
<i>MAP9</i>	cg03616357	0.12	0.60	0.48	9.64E-07
<i>NETO2</i>	cg02755525	0.13	0.59	0.46	5.78E-05
<i>INA</i>	cg25764191	0.16	0.62	0.46	7.22E-07
<i>SPINT2</i>	cg15375239	0.10	0.55	0.45	8.67E-04
<i>AKR1B1</i>	cg13801416	0.06	0.50	0.45	2.87E-07
<i>CDKL2</i>	cg24432073	0.08	0.52	0.45	1.08E-06
<i>RSPH9</i>	cg04600618	0.13	0.57	0.44	1.50E-07
<i>APC</i>	cg16970232	0.20	0.64	0.44	6.98E-04
<i>LDHB</i>	cg06437004	0.13	0.56	0.43	5.64E-06
<i>CDKN2A</i>	cg09099744	0.11	0.55	0.43	2.20E-06
<i>ZFP41</i>	cg12680609	0.14	0.56	0.43	1.75E-06
<i>GSTP1</i>	cg02659086	0.07	0.50	0.43	4.14E-05
<i>FOXE3</i>	cg18815943	0.14	0.57	0.42	3.74E-04
<i>HBQ1</i>	cg07703401	0.18	0.60	0.42	1.11E-06
<i>GRASP</i>	cg04034767	0.12	0.53	0.42	2.20E-06
<i>ABHD9</i>	cg05488632	0.19	0.61	0.42	1.44E-06
<i>BMP4</i>	cg14310034	0.10	0.52	0.41	1.38E-05
<i>SF3B14</i>	cg04809136	0.18	0.60	0.41	8.11E-04
<i>DGKE</i>	cg01344452	0.12	0.53	0.41	8.27E-04
<i>ABCA3</i>	cg00949442	0.20	0.61	0.41	2.33E-05
<i>STEAP4</i>	cg00564163	0.17	0.58	0.41	1.35E-05
<i>POU4F1</i>	cg08097882	0.12	0.53	0.40	7.97E-06
<i>DKFZp434I1020</i>	cg17886204	0.04	0.45	0.40	7.53E-07
<i>NXPE3</i>	cg06073471	0.04	0.44	0.40	1.53E-06
<i>PRDM14</i>	cg01295203	0.15	0.54	0.39	1.09E-06
<i>CCNJ</i>	cg04590978	0.11	0.50	0.39	5.84E-06
<i>SPDY1</i>	cg04786857	0.18	0.58	0.39	2.08E-06
<i>HIST1H4F</i>	cg08260959	0.15	0.54	0.39	9.91E-07

^aTop 30 hypermethylated genes in HCC tumors compared to non-tumor liver tissues ranked by mean β -value difference ($\Delta \beta$); ^bp-value corrected for false discovery rate by the Benjamini-Hochberg method.

coli), *CDKN2A* (cyclin-dependent kinase inhibitor 2A) and *GSTP1* (glutathione S-transferase pi 1), which are known to be silenced by DNA hypermethylation in HCC (14,15), supporting the appropriateness of our methodology.

We examined whether the remaining 27 genes were silenced by DNA hypermethylation in the paired tumor and non-tumor tissues from an additional 27 patients with primary

HCC (the validation set) using MSP and qRT-PCR. Of the 27 genes, eight genes (*AKR1B1*, *GRASP*, *MAP9*, *NXPE3*, *RSPH9*, *SPINT2*, *STEAP4*, and *ZNF154*) were significantly hypermethylated and downregulated in the HCC tumors compared to the non-tumor liver tissues (Fig. 3 and Table V). Therefore, these eight genes were identified and validated to be methylated genes in HCC.

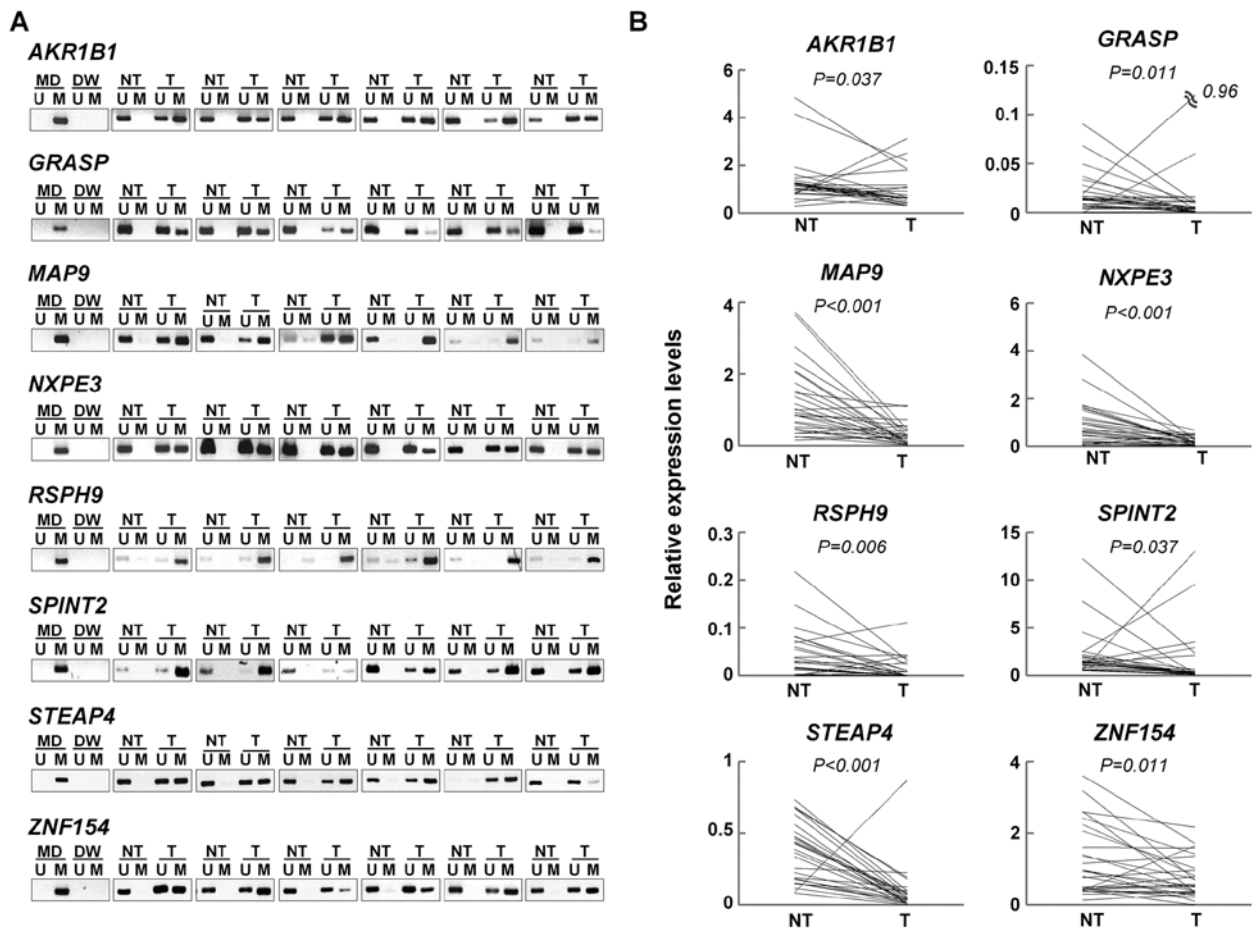


Figure 3. (A) MSP analysis of the indicated eight genes in paired tumor (T) and non-tumor (NT) tissues from representative six patients with primary HCC. Parallel amplification reactions were performed using primers specific for unmethylated (U) or methylated (M) DNA. Methylated DNA (MD) was used as controls. DW is a deionized water control. (B) Relative expression levels of the indicated eight genes in paired tumor (T) and non-tumor (NT) tissues from 27 patients with primary HCC as evaluated by qRT-PCR. Comparisons were made using the Wilcoxon signed-rank test.

Table V. Methylation-specific PCR analysis of candidate genes.

Gene	Non-tumor (n=27)	Tumor (n=27)	P-value ^a
<i>AKR1B1</i>	1 (4)	20 (74)	<0.001
<i>GRASP</i>	0 (0)	12 (44)	<0.001
<i>MAP9</i>	11 (41)	25 (93)	<0.001
<i>NXPE3</i>	2 (7)	21 (78)	<0.001
<i>RSPH9</i>	10 (37)	26 (96)	<0.001
<i>SPINT2</i>	0 (0)	15 (56)	<0.001
<i>STEAP4</i>	10 (37)	23 (85)	<0.001
<i>ZNF154</i>	2 (7)	23 (85)	<0.001

Values are the number (%) of the methylation-positive samples. ^aFisher's exact probability test.

Epigenetic silencing of *STEAP4*. As an example, we further assessed the methylation status of *STEAP4*, as little is known about the association of *STEAP4* with HCC. Using the Methyl Primer Express software ver.1.0 (Applied Biosystems, Foster City, CA, USA), a CpG island was found around the transcription start site of *STEAP4* (Fig. 4A). To confirm the

methylation status of *STEAP4*, we quantified methylation levels of *STEAP4* in the paired tumor and non-tumor tissues from 27 patients with primary HCC (the validation set) using COBRA (Fig. 4B). The level of methylation of *STEAP4* was significantly higher in 25 (93%) of the 27 HCC tumors, compared to their non-tumor tissue counterparts (Wilcoxon signed-rank test, $P<0.001$) (Fig. 4C).

To confirm the silencing of *STEAP4* in the HCC tumors, we compared the expression of the *STEAP4* protein using immunohistochemistry on tissue microarrays. Representative images are shown in Fig. 4D. Whereas the *STEAP4* protein was expressed in all of the 30 non-tumor liver tissues, it was expressed in 26 of the 40 HCC tumors (Fisher's exact probability test, $P<0.001$).

We then assessed the effect of demethylation on the expression of *STEAP4*. Three HCC cell lines (SNU449, Li7, and HLF) that lack *STEAP4* expression were treated with 5-aza-dC, a methyltransferase inhibitor, and expression levels of *STEAP4* mRNA were assayed with qRT-PCR. Expression of *STEAP4* was restored with 5-aza-dC treatment in a dose-dependent manner in all three HCC cells (Fig. 4E), suggesting that aberrant DNA methylation suppressed the expression of *STEAP4*. Additionally, it was observed that treatment with a histone deacetylase inhibitor, TSA, enhanced the expression of *STEAP4* by 5-aza-dC in all three cell lines (Fig. 4E). This

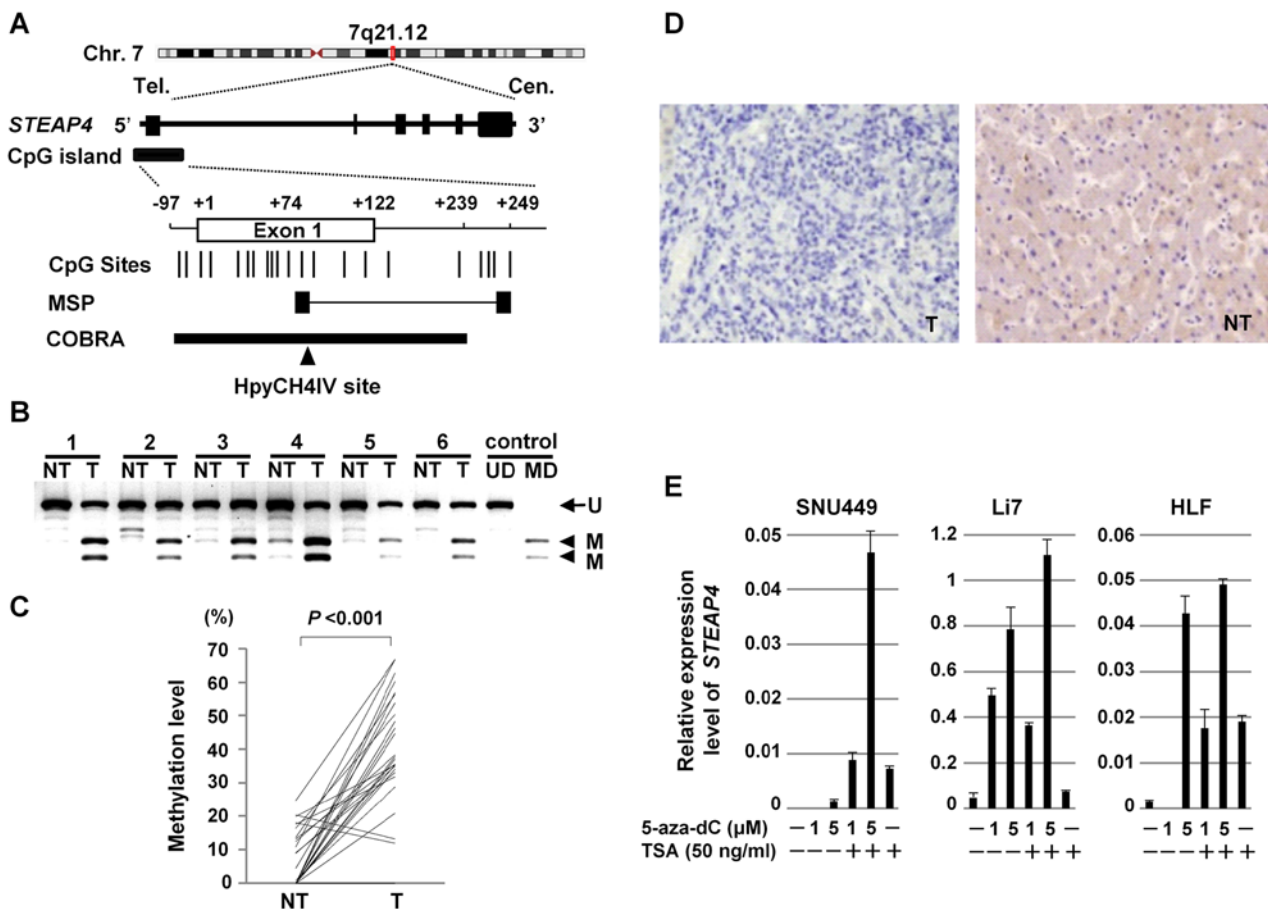


Figure 4. Epigenetic silencing of *STEAP4*. (A) Schematic map of the CpG island extending into exon 1 of *STEAP4*. Exon 1 is indicated by an open box, and the transcription start site is marked at +1. CpG sites are indicated by vertical ticks. The regions selected for MSP (Fig. 3A) and COBRA are indicated. The restriction site for HpyCH4IV is indicated by the black arrowhead. (B) COBRA of *STEAP4* in paired tumor (T) and non-tumor (NT) tissues from representative six patients with primary HCC. The arrow and arrowheads indicate undigested products (unmethylated DNA, U) and digested fragments (methylated DNA, M), respectively. Unmethylated DNA (UD) and methylated DNA (MD) were used as controls. (C) Plot of the methylation levels of *STEAP4* in paired tumors and non-tumor tissues from 27 patients with primary HCCs. Methylation levels were determined by COBRA, as described in Materials and methods, and were expressed as a percentage of the methylated DNA-positive control value. The value obtained for the unmethylated DNA control was used as the baseline (0%). (D) Representative immunostaining of *STEAP4* protein in paired tumor (T) and non-tumor (NT) tissues from representative two patients with primary HCC. (E) Effects of 5-aza-dC and TSA treatment on the expression of *STEAP4*. Expression levels of *STEAP4* mRNA were determined by qRT-PCR in three HCC cell lines (SNU449, Li7, and HLF) with or without treatment with 5-aza-dC (1 or 5 μ M) for 4 days and/or TSA (50 ng/ml) for 24 h.

finding suggests that histone deacetylation may also contribute to the transcriptional repression of *STEAP4*.

Discussion

In the present study, *AKR1B1*, *GRASP*, *MAP9*, *NXPE3*, *RSPH9*, *SPINT2*, *STEAP4* and *ZNF154* were identified as genes that are silenced by DNA hypermethylation in HCC. Except for *GRASP* and *SPINT2*, to our knowledge, this is the first study to describe the hypermethylation of *AKR1B1*, *MAP9*, *NXPE3*, *RSPH9*, *STEAP4* and *ZNF154* in HCC and the relevance of these genes with HCC. Our methodology appears to be appropriate, since *APC*, *CDKN2A* and *GSTP1*, which are known methylated genes in HCC, were also identified by our approach.

GRASP [GRP1 (general receptor for phosphoinositides 1)-associated scaffold protein; also known as Tamalin] encodes a protein that functions as a molecular scaffold and contains several putative protein-protein interaction motifs. It regulates the membrane trafficking pathway (16,17). Although a recent study showed the hypermethylation of *GRASP* in

hepatitis B-virus related HCC (18), its functional relevance for the development of HCC remains unknown.

SPINT2 (serine peptidase inhibitor, Kunitz type, 2) encodes Kunitz-type serine protease inhibitor called hepatocyte growth factor activator inhibitor type 2 (HAI-2). Recent studies have suggested that *SPINT2* is a candidate tumor-suppressor gene that is frequently hypermethylated and underexpressed in human cancers, including hepatocellular carcinomas (19,20), gastric carcinomas (21), ovarian cancer (22), cervical cancer (23), renal cell carcinoma (24), and esophageal squamous cell carcinoma (25). Studies showed that ectopic expression of *SPINT2* significantly inhibited cell migration and invasiveness of HCC cells *in vitro* and suppressed tumorigenicity *in vivo* (20).

AKR1B1 (aldo-keto reductase family 1, member B1) encodes aldose reductase, which participates in glucose metabolism and osmoregulation and is believed to play a protective role against toxic aldehydes derived from lipid peroxidation and steroidogenesis. *AKR1B1* is mainly expressed in the adrenal gland and its expression is decreased in adrenocortical cancer (26).

STEAP4 (STEAP family member 4), also known as STAMP2, is a member of the six transmembrane epithelial antigen of prostate (STEAP) family and functions as a metalloredutase. STEAP4 is involved in adipocyte development and metabolism, and it is essential for maintenance of systemic metabolic homeostasis (27). Studies suggest that STEAP4 may contribute to normal physiology of the prostate as well as prostate cancer progression. STEAP4 was reported to be overexpressed in primary prostate cancer (28), whereas it was also reported that the STEAP4 promoter region is methylated in androgen-independent prostate cancer cells, but not in androgen-dependent prostate cancer cells (29).

ZNF154 (zinc finger protein 154) encodes a protein that belongs to the zinc finger Kruppel family of transcriptional regulators. Although the function of *ZNF154* is unknown, hypermethylation of this gene was recently reported in bladder cancer (30) and ovarian cancer (31).

MAP9 (microtubule-associated protein 9; also known as ASAP) is a microtubule-associated protein required for spindle function, mitotic progression, and cytokinesis (32). Expression of MAP9 is downregulated in colorectal cancer compared to normal tissues (33). *RSPH9* (radial spoke head 9 homolog) encodes a protein thought to be a component of the radial spoke head in motile cilia and flagella. Mutations in this gene have been found in patients with primary ciliary dyskinesia (34). However, the relevance of *RSPH9* with cancer has not been reported. The function of *NXPE3* (neurexophilin and PC-esterase domain family, member 3) is unknown.

Of these eight genes, we further examine the methylation status of *STEAP4* using a variety of methods, including COBRA and the treatment with a methyltransferase inhibitor and a histone deacetylase inhibitor. We confirmed the hypermethylation of the promoter region of *STEAP4* in HCC. Moreover, qRT-PCR and immunohistochemistry showed that the expression of *STEAP4* was downregulated at the mRNA and protein levels in HCC. These combined results suggest that the silencing of *STEAP4* by aberrant promoter hypermethylation may be associated with the development and progression of HCC. We are now going to study the relationship between the reduced expression of *STEAP4* in HCC tumors and clinicopathological features with a larger number of samples. It is also required to study the functional role of *STEAP4* in hepatocarcinogenesis.

Our pathway analysis suggested that hypermethylated genes may be involved in the pathways of neuroactive ligand-receptor interaction, focal adhesion, vascular smooth muscle contraction, and systemic lupus erythematosus in HCC. However, the relevance of hypermethylated genes with these pathways is largely unknown.

Functional studies are needed to clarify the roles of hypermethylated genes that were identified in the present study in the development and progression of HCC, as they could be useful markers for the diagnosis or be targets for the therapy of HCCs.

References

1. Ferlay J, Shin HR, Bray F, Forman D, Mathers C and Parkin DM: Estimates of worldwide burden of cancer in 2008: GLOBOCAN 2008. *Int J Cancer* 127: 2893-2917, 2010.
2. Lou C, Du Z, Yang B, Gao Y, Wang Y and Fang S: Aberrant DNA methylation profile of hepatocellular carcinoma and surgically resected margin. *Cancer Sci* 100: 996-1004, 2009.
3. Matsuda Y, Ichida T, Matsuzawa J, Sugimura K and Asakura H: p16(INK4) is inactivated by extensive CpG methylation in human hepatocellular carcinoma. *Gastroenterology* 116: 394-400, 1999.
4. Zhang YJ, Ahsan H, Chen Y, Lunn RM, Wang LY, Chen SY, Lee PH, Chen CJ and Santella RM: High frequency of promoter hypermethylation of RASSF1A and p16 and its relationship to aflatoxin B1-DNA adduct levels in human hepatocellular carcinoma. *Mol Carcinog* 35: 85-92, 2002.
5. Tchou JC, Lin X, Freije D, Isaacs WB, Brooks JD, Rashid A, De Marzo AM, Kanai Y, Hirohashi S and Nelson WG: GSTP1 CpG island DNA hypermethylation in hepatocellular carcinomas. *Int J Oncol* 16: 663-676, 2000.
6. Calvisi DF, Ladu S, Gorden A, Farina M, Lee JS, Conner EA, Schroeder I, Factor VM and Thorgeirsson SS: Mechanistic and prognostic significance of aberrant methylation in the molecular pathogenesis of human hepatocellular carcinoma. *J Clin Invest* 117: 2713-2722, 2007.
7. Nishida N, Kudo M, Nagasaka T, Ikai I and Goel A: Characteristic patterns of altered DNA methylation predict emergence of human hepatocellular carcinoma. *Hepatology* 56: 994-1003, 2012.
8. Benjamini Y and Hochberg Y: Controlling the false discovery rate: A practical and powerful approach to multiple testing. *J R Stat Soc Series B Stat Methodol* 57: 289-300, 1995.
9. Zen K, Yasui K, Nakajima T, Zen Y, Zen K, Gen Y, Mitsuyoshi H, Minami M, Mitsufuji S, Tanaka S, *et al*: ERK5 is a target for gene amplification at 17p11 and promotes cell growth in hepatocellular carcinoma by regulating mitotic entry. *Genes Chromosomes Cancer* 48: 109-120, 2009.
10. Dohi O, Yasui K, Gen Y, Takada H, Endo M, Tsuji K, Konishi C, Yamada N, Mitsuyoshi H, Yagi N, *et al*: Epigenetic silencing of miR-335 and its host gene MEST in hepatocellular carcinoma. *Int J Oncol* 42: 411-418, 2013.
11. Kanehisa M and Goto S: KEGG: Kyoto encyclopedia of genes and genomes. *Nucleic Acids Res* 28: 27-30, 2000.
12. Huang W, Sherman BT and Lempicki RA: Systematic and integrative analysis of large gene lists using DAVID bioinformatics resources. *Nat Protoc* 4: 44-57, 2009.
13. Huang W, Sherman BT and Lempicki RA: Bioinformatics enrichment tools: Paths toward the comprehensive functional analysis of large gene lists. *Nucleic Acids Res* 37: 1-13, 2009.
14. Nishida N, Nagasaka T, Nishimura T, Ikai I, Boland CR and Goel A: Aberrant methylation of multiple tumor suppressor genes in aging liver, chronic hepatitis, and hepatocellular carcinoma. *Hepatology* 47: 908-918, 2008.
15. Edamoto Y, Hara A, Biernat W, Terracciano L, Cathomas G, Riehle HM, Matsuda M, Fujii H, Scoazec JY and Ohgaki H: Alterations of RB1, p53 and Wnt pathways in hepatocellular carcinomas associated with hepatitis C, hepatitis B and alcoholic liver cirrhosis. *Int J Cancer* 106: 334-341, 2003.
16. Sugi T, Oyama T, Muto T, Nakanishi S, Morikawa K and Jingami H: Crystal structures of autoinhibitory PDZ domain of Tamalin: Implications for metabotropic glutamate receptor trafficking regulation. *EMBO J* 26: 2192-2205, 2007.
17. Venkataraman A, Nevriy DJ, Filtz TM and Leid M: Grp1-associated scaffold protein (GRASP) is a regulator of the ADP ribosylation factor 6 (Arf6)-dependent membrane trafficking pathway. *Cell Biol Int* 36: 1115-1128, 2012.
18. Tao R, Li J, Xin J, Wu J, Guo J, Zhang L, Jiang L, Zhang W, Yang Z and Li L: Methylation profile of single hepatocytes derived from hepatitis B virus-related hepatocellular carcinoma. *PLoS One* 6: e19862, 2011.
19. Fukui K, Yokosuka O, Chiba T, Hirasawa Y, Tada M, Imazeki F, Kataoka H and Saisho H: Hepatocyte growth factor activator inhibitor 2/placental bikunin (HAI-2/PB) gene is frequently hypermethylated in human hepatocellular carcinoma. *Cancer Res* 63: 8674-8679, 2003.
20. Tung EK, Wong CM, Yau TO, Lee JM, Ching YP and Ng IO: HAI-2 is epigenetically downregulated in human hepatocellular carcinoma, and its Kunitz domain type 1 is critical for anti-invasive functions. *Int J Cancer* 124: 1811-1819, 2009.
21. Dong W, Chen X, Xie J, Sun P and Wu Y: Epigenetic inactivation and tumor suppressor activity of HAI-2/SPINT2 in gastric cancer. *Int J Cancer* 127: 1526-1534, 2010.
22. Nakamura K, Abarzua F, Kodama J, Hongo A, Nasu Y, Kumon H and Hiramatsu Y: Expression of hepatocyte growth factor activator inhibitors (HAI-1 and HAI-2) in ovarian cancer. *Int J Oncol* 34: 345-353, 2009.

23. Nakamura K, Abarzua F, Hongo A, Kodama J, Nasu Y, Kumon H and Hiramatsu Y: Hepatocyte growth factor activator inhibitor-2 (HAI-2) is a favorable prognosis marker and inhibits cell growth through the apoptotic pathway in cervical cancer. *Ann Oncol* 20: 63-70, 2009.
24. Morris MR, Gentle D, Abdulrahman M, Maina EN, Gupta K, Banks RE, Wiesener MS, Kishida T, Yao M, Teh B, *et al*: Tumor suppressor activity and epigenetic inactivation of hepatocyte growth factor activator inhibitor type 2/SPINT2 in papillary and clear cell renal cell carcinoma. *Cancer Res* 65: 4598-4606, 2005.
25. Yue D, Fan Q, Chen X, Li F, Wang L, Huang L, Dong W, Chen X, Zhang Z, Liu J, *et al*: Epigenetic inactivation of SPINT2 is associated with tumor suppressive function in esophageal squamous cell carcinoma. *Exp Cell Res* 322: 149-158, 2014.
26. Lefrançois-Martinez AM, Bertherat J, Val P, Tournaire C, Gallo-Payet N, Hyndman D, Veyssière G, Bertagna X, Jean C and Martinez A: Decreased expression of cyclic adenosine monophosphate-regulated aldose reductase (AKR1B1) is associated with malignancy in human sporadic adrenocortical tumors. *J Clin Endocrinol Metab* 89: 3010-3019, 2004.
27. Wellen KE, Fucho R, Gregor MF, Furuhashi M, Morgan C, Lindstad T, Vaillancourt E, Gorgun CZ, Saatcioglu F and Hotamisligil GS: Coordinated regulation of nutrient and inflammatory responses by STAMP2 is essential for metabolic homeostasis. *Cell* 129: 537-548, 2007.
28. Korkmaz CG, Korkmaz KS, Kurys P, Elbi C, Wang L, Klock TI, Hammarstrom C, Troen G, Svindland A, Hager GL, *et al*: Molecular cloning and characterization of STAMP2, an androgen-regulated six transmembrane protein that is overexpressed in prostate cancer. *Oncogene* 24: 4934-4945, 2005.
29. Tamura T and Chiba J: STEAP4 regulates focal adhesion kinase activation and CpG motifs within STEAP4 promoter region are frequently methylated in DU145, human androgen-independent prostate cancer cells. *Int J Mol Med* 24: 599-604, 2009.
30. Reinert T, Borre M, Christiansen A, Hermann GG, Ørntoft TF and Dyrskjød L: Diagnosis of bladder cancer recurrence based on urinary levels of EOMES, HOXA9, POU4F2, TWIST1, VIM, and ZNF154 hypermethylation. *PLoS One* 7: e46297, 2012.
31. Sánchez-Vega F, Gotea V, Petrykowska HM, Margolin G, Krivak TC, DeLoia JA, Bell DW and Elnitski L: Recurrent patterns of DNA methylation in the ZNF154, CASP8, and VHL promoters across a wide spectrum of human solid epithelial tumors and cancer cell lines. *Epigenetics* 8: 1355-1372, 2013.
32. Saffin JM, Venoux M, Prigent C, Espeut J, Poulat F, Giorgi D, Abrieu A and Rouquier S: ASAP, a human microtubule-associated protein required for bipolar spindle assembly and cytokinesis. *Proc Natl Acad Sci USA* 102: 11302-11307, 2005.
33. Rouquier S, Pillaire MJ, Cazaux C and Giorgi D: Expression of the microtubule-associated protein MAP9/ASAP and its partners AURKA and PLK1 in colorectal and breast cancers. *Dis Markers* 2014: 798170, 2014.
34. Castleman VH, Romio L, Chodhari R, Hirst RA, de Castro SC, Parker KA, Ybot-Gonzalez P, Emes RD, Wilson SW, Wallis C, *et al*: Mutations in radial spoke head protein genes RSPH9 and RSPH4A cause primary ciliary dyskinesia with central-microtubular-pair abnormalities. *Am J Hum Genet* 84: 197-209, 2009.